Aust. J. Math. Anal. Appl.
Vol. **21** (2024), No. 1, Art. 13, 20 pp.
AJMAA

FINITE VOLUME APPROXIMATION OF A CLASS OF 2D ELLIPTIC EQUATIONS WITH DISCONTINUOUS AND HIGHLY OSCILLATING COEFFICIENTS

J. D. BAMBI PEMBA AND B. ONDAMI

Received 14 January, 2024; accepted 22 April, 2024; published 31 May, 2024.

UNIVERSITÉ MARIEN NGOUABI, FACTUTÉ DES SCIENCES ET TECHNIQUES, BP 69, BRAZZAVILLE, CONGO.
bondami@gmail.com
URL: https://www.researchgate.net/profile/Bienvenu-Ondami
https://www.linkedin.com/in/bienvenu-ondami

ABSTRACT. In this paper, we are interested in the Finite Volume approximation of a second-order two-dimensional elliptic equation in heterogeneous porous medium with a periodic structure. The equation's coefficients are therefore discontinuous and highly oscillating. This class of problems has been extensively studied in the literature, where various methods proposed for determining the so-called homogenized problem. What we are particularly interested in is the direct numerical approximation of the problem, which has received little attention in the literature. We use the cell-centered finite volume approach for this purpose. Error estimates are established, and numerical simulations are conducted for both the isotropic and anisotropic media cases. The obtained solution is compared to the homogenized solution, and the results show that this approach provides an adequate approximation of the exact solution.

Key words and phrases: Homogenization; Elliptic Equations; Finite Volume Method; Porous Medium.

2010 *Mathematics Subject Classification.* 65N08, 35B27, 35J15.

ISSN (electronic): 1449-5910

1. INTRODUCTION

There exist numerous practical computational problems that have solutions with highly oscillatory behavior, such as the computation of flow in heterogeneous porous media for petroleum and groundwater reservoir simulation (see, for example, [15] and the bibliographies therein). If we consider a porous medium with periodic structure, where the period size is much smaller than the size of the reservoir, denoted by ε $(0 < \varepsilon << 1)$, an asymptotic analysis as ε approaches 0 is necessary. We will consider the following model problem:

$$(P_\varepsilon) \qquad \begin{cases} -\mathrm{div}\left(K^\varepsilon(x)\nabla u^\varepsilon\right) &= f \quad \text{in } \Omega, \\ u_\varepsilon &= 0 \quad \text{on } \Gamma. \end{cases}$$

$\Omega \subset \mathsf{R}^n$ $(n = 1, 2, 3)$ is a bounded polygonal convex domain with a periodic structure and smooth boundary Γ, $K^\varepsilon(x) = K(x/\varepsilon)$, K is a symmetric and uniformly positive definite matrix in Ω which has discontinuities across a given interface. The case of piecewise constant coefficient K^ε is very important for the applications.

In porous medium flow, the problem (P_ε) results from Darcy's law and continuity for a single phase, incompressible flow through a horizontal heterogeneous porous medium with periodic structure.

Using homogenization tools (see e.g. [5], [6], [17], [24]), the original problem (P_ε) can be replaced by a homogenized problem that models some average quantity without the oscillations. Homogenized equations are extremely useful for computational purposes whenever they are applicable. This theory is applicable to models with highly oscillating coefficients so that the examples with $\varepsilon = 1/2$, $\varepsilon = 1/4$, ... are beyond the framework.

The numerical approximation of partial differential equations with highly oscillating coefficients has been a topic of interest for many years, with various methods developed (see, for example, [2], [10], [20], [21], [22], [27] and the references therein).

The case in which K^ε has continuous coefficients has been extensively studied. Some studies have also examined the situation involving discontinuous coefficients, such as in [7] and [8], where the authors analyze the 1D problem by investigating specific correctors derived from the asymptotic expansion in order to obtain a suitable approximation of the exact solution. In [2] and [22], the numerical approximation of the problem with discontinuous coefficients was carried out using finite element methods, no error estimate has been established and remains an unresolved issue to the best of our knowledge.

The approximation of the problem with discontinuous coefficients by a finite volume method has only been approached recently in [20], only in 1D case, where errors estimates are established.

The elliptic problems with discontinuous coefficients (referred to as interface problems) naturally arise in mathematical modeling processes involving heat and mass transfer, diffusion in composite media, flows in porous media, etc.

In this paper, the approximation is performed using a cell-centered finite volume method (see, for example, [11], [12], [13], [14]), focusing on the two-dimensional problem ($2D$ problem). The numerical simulations are carried out using the homogenized solution as a reference solution.

The paper is organized as follows: Section 2 presents a description of the methods employed as well as the error estimates obtained. Section 3 is dedicated to numerical simulations. Finally, some concluding remarks are presented in Section 4.

2. FINITE VOLUME APPROXIMATION

We will focus to the case where K^ε is a diagonal matrix with piecewise constant coefficients, and we will assume that $\Omega = (0,1) \times (0,1)$. In this case the problem (P_ε) can be simply written as follows:

$$\left\{ \begin{array}{l} -\left(K_{11}^\varepsilon u_x^\varepsilon\right)_x - \left(K_{22}^\varepsilon u_y^\varepsilon\right)_y = f(x,y) \quad \text{in } \Omega, \\ u^\varepsilon(0,y) = u^\varepsilon(x,0) = u^\varepsilon(1,y) = u^\varepsilon(x,1) = 0. \end{array} \right. \tag{2.1}$$

where $K_{ll}^\varepsilon(x) = K_{ll}\left(x / \varepsilon\right) = K_{ll}(y)$, with $y = x / \varepsilon$, $K_{ll}(l = 1,2)$ are piecewise constant (see [4] for the case of piecewise continuous functions) and periodic functions of period 1 on $(0,1) \times (0,1)$. In all of this paper we make the following assumptions:

$(A1)$ $\alpha < K^\varepsilon(x)\xi.\xi \leq \beta$ for $a.e.\ x \in \Omega$ and $\forall\, \xi \in \mathsf{R}^2,$ with some $\alpha, \beta \in \mathsf{R}_+^*$.

$(A2)$ $f \in L^2\left(]\Omega[\right)$.

It is well known that assumptions $(A1)$ and $(A2)$ ensure the existence and uniqueness of the solution of the problem (2.1). From homogenization theory (see e.g. [6, 17, 24]) follows:

$$u_\varepsilon \rightharpoonup u \quad \text{in} \quad H_0^1\left(\Omega\right) \text{(consists of functions in Sobolev space } H^1\left(\Omega\right) \text{ that vanish on } \Gamma)$$

weakly, where u (homogenized solution) satisfies the following homogenized problem:

$$\left\{ \begin{array}{rcll} -\mathrm{div}\left(K^*\left(x\right)\nabla u\right) & = & f & \text{in } \Omega, \\ u & = & 0 & \text{on } \Gamma. \end{array} \right. \tag{2.2}$$

Tensor K^* is called effective (or homogenized) and calculed by solving the so-called local or cell problem. He is still symmetric and positive definite, but in general cases, even with the permeability at the microscopic scale in the porous medium being isotropic, we may have an effective tensor which is significantly anisotropic (see e.g. [1]).
We are interested here in the approximation of (1) by a cell-centenred finite volume method. In order to do this, let us define a Ω mesh, denoted by Ω_h, satisfying the following definition.

Definition 2.1. Let be Ω_h an uniform mesh of Ω given by partitioning Ω in the x and y directions as:
$0 = x_{\frac{1}{2}} < x_1 < x_{\frac{3}{2}} < x_2 < ... < x_{i-\frac{1}{2}} < x_i < x_{N+\frac{1}{2}} = 1,$
$0 = y_{\frac{1}{2}} < y_1 < y_{\frac{3}{2}} < y_2 < ... < y_{j-\frac{1}{2}} < y_i < y_{N+\frac{1}{2}} = 1.$
We then define the cells (finite volumes) to be the square
$V_{i,j} = \left(x_{i-\frac{1}{2}}, x_{i+\frac{1}{2}}\right) \times \left(y_{j-\frac{1}{2}}, y_{j+\frac{1}{2}}\right), 1 \leq i,j \leq N$, with the center (x_i, y_j) and nodes of half indices. Let be

$$h = x_{i+1} - x_i = y_{j+1} - y_j,\ 1 \leq i,j \leq N-1,\ h = x_{i+\frac{1}{2}} - x_{i-\frac{1}{2}} = y_{i+\frac{1}{2}} - y_{i-\frac{1}{2}},\ 1 \leq i,j \leq N.$$

Ω_h is then defined as follows:

$$\Omega_h = \{\ V_{i,j},\ \ 1 \leq i,j \leq N\},\ \text{ with } \ V_{i,j} \ \text{ as in the below graphic} \tag{2.3}$$

Ω_h is an admissible mesh of Ω in the sens of Definitions 3.1 and 3.7 which are in [13] (pp. 37 & 79).

Figure 1: Cells graphics

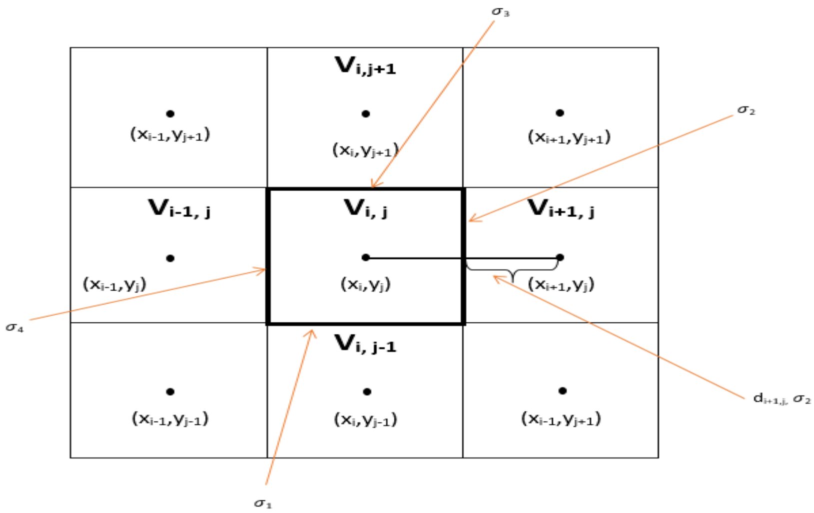

2.1. **Cell-Centered Finite Volume Distcretization.** The cell-centered finite volume approximation consists in seeking a discrete approximate solution vector whose each component $u^{\varepsilon}_{i,j} \approx u^{\varepsilon}(x_i, x_j)$, is constant on each volume $V_{i,j}$.
Let Ω_h be an admissible mesh, in the sense of Definition 2.1, such that the discontinuities of tensor K^{ε} coincide with the mesh interfaces. The principle of classical finite volume schemes is to integrate the first equation of the problem (2.1) on each volume of the mesh $V_{i,j}$ (see e.g. [13]). So by using divergence formula to integrate the first equation of (2.1) on each $V_{i,j}$, one has:

$$\sum_{\sigma \in \partial V_{i,j}} -\int_{\sigma} K^{\varepsilon}(x)\nabla u^{\varepsilon}(x).n_{V_{i,j},\sigma} d\gamma(x) = \int_{V_{i,j}} f(x)dx \tag{2.4}$$

where $\partial V_{i,j}$ denotes the set of edges of the control volume $V_{i,j}$ and σ is any edge. $n_{V_{i,j},\sigma}$ is the normal unit vector to σ outward to $V_{i,j}$ and $d\gamma$ denotes the integration symbol for the onedimensional Lebesgue mesure. The finite volume scheme for the numerical approximation of the solution of Problem (2.1) is obtained by approximating the flux over each edge σ of $V_{i,j}$. This yields:

$$\sum_{\sigma \in \partial V_{i,j}} F^{\varepsilon}_{V_{i,j},\sigma} = m(V_{i,j}) f_{ij}, \tag{2.5}$$

where $f_{ij} = \frac{1}{m(V_{i,j})} \int_{V_{i,j}} f(x)dx$ and $F^{\varepsilon}_{V_{i,j},\sigma}$ is an approximation of

$$\int_{\sigma} -K^{\varepsilon}_{V_{i,j}} \nabla u^{\varepsilon}(x).n_{V_{i,j},\sigma} d\gamma(x),\ K^{\varepsilon}_{V_{i,j}} = \frac{1}{m\left(V_{i,j}\right)} \int_{V_{i,j}} K^{\varepsilon}\left(x\right) dx.$$

So, from (2.5) and using Figure 1, one has:

$$F_{V_{i,j},\sigma_1} + F_{V_{i,j},\sigma_2} + F_{V_{i,j},\sigma_3} + F_{V_{i,j},\sigma_4} = m(V_{i,j}) f_{ij}, \tag{2.6}$$

where [13]:

$$F_{V_{i,j},\sigma_k} = -m(\sigma_m)\lambda^{\varepsilon}_{V_{i,j},\sigma_m} \frac{u^{\varepsilon}_{\sigma_m} - u^{\varepsilon}_{ij}}{d_{i,j,\sigma_m}},\ 1 \le m \le 4,\ 2 \le i,j \le N-1, \tag{2.7}$$

$$\lambda^{\varepsilon}_{V_{i,j},\sigma_m} = |K^{\varepsilon}_{V_{i,j}}.n_{V_{i,j},\sigma_m}|\ \ (|.|\text{ denotes the Eucludean norm}), \tag{2.8}$$

$$m(\sigma_m) = h\,(\text{uniform mesh})\,,\ d_{i,j,\sigma_m} = \frac{h}{2}. \tag{2.9}$$

Writting the conservativity of the scheme (see [13]) between $V_{i,j}$ and $V_{i+1,j}$ i.e. $F_{V_{i+1,j},\sigma_2} = -F_{V_{i,j},\sigma_2}$, we get:

$$u^{\varepsilon}_{\sigma_2} = \frac{\lambda^{\varepsilon}_{V_{ij},\sigma_2} d_{i+1,j,\sigma_2} u^{\varepsilon}_{ij} + \lambda^{\varepsilon}_{V_{i+1,j},\sigma_2} d_{i,j,\sigma_2} u^{\varepsilon}_{i+1,j}}{\lambda^{\varepsilon}_{V_{ij},\sigma_2} d_{i+1,j,\sigma_2} + \lambda^{\varepsilon}_{V_{i+1,j},\sigma_2} d_{i,j,\sigma_2}}. \tag{2.10}$$

From (2.8) one has:

$$\lambda^{\varepsilon}_{V_{i,j},\sigma_2} = K^{i,j,\varepsilon}_{11},\ \ \lambda^{\varepsilon}_{V_{i+1,j},\sigma_2} = K^{i+1,j,\varepsilon}_{11}, \tag{2.11}$$

where $K^{i,j,\varepsilon}_{11}$ and $K^{i+1,j,\varepsilon}_{11}$ are the K^{ε}_{11} values on $V_{i,j}$ and $V_{i+1,j}$ respectively. Using (2.7), (2.10) and (2.11), we get :

$$F_{V_{ij},\sigma_2} = \tau^{\varepsilon}_{i+1,j,\sigma_2}(u^{\varepsilon}_{ij} - u^{\varepsilon}_{i+1,j}), \tag{2.12}$$

where

$$\tau^{\varepsilon}_{i+1,j,\sigma_2} = \tau^{i+1,j}_{11,\varepsilon} = \frac{2K^{i,j,\varepsilon}_{11} K^{i+1,j,\varepsilon}_{11}}{K^{i,j,\varepsilon}_{11} + K^{i+1,j,\varepsilon}_{11}}. \tag{2.13}$$

In the same way we get:

$$F_{V_{ij},\sigma_1} = \tau^{\varepsilon}_{i,j-1,\sigma_1}(u^{\varepsilon}_{i,j} - u^{\varepsilon}_{i,j-1}), \tag{2.14}$$

$$F_{V_{ij},\sigma_3} = \tau^{\varepsilon}_{i,j+1,\sigma_3}(u^{\varepsilon}_{ij} - u^{\varepsilon}_{i,j+1}), \tag{2.15}$$

$$F_{V_{ij},\sigma_4} = \tau^{\varepsilon}_{i-1,j,\sigma_4}(u^{\varepsilon}_{i,j} - u^{\varepsilon}_{i-1,j}), \tag{2.16}$$

where

$$\tau^{\varepsilon}_{i,j-1,\sigma_1} = \tau^{i,j-1}_{22,\varepsilon} = \frac{2K^{i,j,\varepsilon}_{22} K^{i,j-1,\varepsilon}_{22}}{K^{i,j,\varepsilon}_{22} + K^{i,j-1,\varepsilon}_{22}}, \tag{2.17}$$

$$\tau^{\varepsilon}_{i,j+1,\sigma_3} = \tau^{i,j+1}_{22,\varepsilon} = \frac{2K^{i,j,\varepsilon}_{22} K^{i,j+1,\varepsilon}_{22}}{K^{i,j,\varepsilon}_{22} + K^{i,j+1,\varepsilon}_{22}}, \tag{2.18}$$

$$\tau^{\varepsilon}_{i-1,j,\sigma_4} = \tau^{i-1,j}_{11,\varepsilon} = \frac{2K^{i,j,\varepsilon}_{11} K^{i-1,j,\varepsilon}_{11}}{K^{i,j,\varepsilon}_{11} + K^{i-1,j,\varepsilon}_{11}}. \tag{2.19}$$

from (2.6)-(2.19) we get for $2 \leq i,j \leq N-1$ (internal cells):

$$\begin{aligned}\tau^{i-1,j}_{11,\varepsilon}\left(u^{\varepsilon}_{i,j} - u^{\varepsilon}_{i-1,j}\right) - \tau^{i+1,j}_{11,\varepsilon}\left(u^{\varepsilon}_{i+1,j} - u^{\varepsilon}_{i,j}\right) + \tau^{i,j-1}_{22,\varepsilon}\left(u^{\varepsilon}_{i,j} - u^{\varepsilon}_{i,j-1}\right) - \tau^{i,j+1}_{22,\varepsilon}\left(u^{\varepsilon}_{i,j+1} - u^{\varepsilon}_{i,j}\right)\\ = h^2 f_{i,j}.\end{aligned} \tag{2.20}$$

From (2.20), and after grouping similar terms, we get for $2 \leq i,j \leq N-1$:

$$-\tau^{i-1,j}_{11,\varepsilon}u^{\varepsilon}_{i-1,j} - \tau^{i,j-1}_{22,\varepsilon}u^{\varepsilon}_{i,j-1} - \tau^{i+1,j}_{11,\varepsilon}u^{\varepsilon}_{i+1,j} - \tau^{i,j+1}_{22,\varepsilon}u^{\varepsilon}_{i,j+1} + \left(\tau^{i-1,j}_{11,\varepsilon} + \tau^{i,j-1}_{22,\varepsilon} + \tau^{i+1,j}_{11,\varepsilon} + \tau^{i,j+1}_{22,\varepsilon}\right)u^{\varepsilon}_{i,j} = h^2 f_{i,j}. \tag{2.21}$$

To complete the scheme (2.21), we need to take boundary edges into account . In the case where one of edges $\sigma_1, \sigma_2, \sigma_3, \sigma_4$ is a boundary edge, one has [13]:

$$F_{V_{i,j},\sigma_1} = m(\sigma_1)\lambda^{\varepsilon}_{V_{i,j},\sigma_1}\frac{u^{\varepsilon}_{i,j}}{d_{i,j,\sigma_1}} = \tau^{i,j}_{22,\varepsilon}u^{\varepsilon}_{i,j}, \ \ \tau^{i,j}_{22,\varepsilon} = 2K^{i,j,\varepsilon}_{22}. \tag{2.22}$$

$$F_{V_{i,j},\sigma_2} = m(\sigma_2)\lambda^{\varepsilon}_{V_{i,j},\sigma_2}\frac{u^{\varepsilon}_{i,j}}{d_{i,j,\sigma_2}} = \tau^{i,j}_{11,\varepsilon}u^{\varepsilon}_{i,j}, \ \ \tau^{i,j}_{11,\varepsilon} = 2K^{i,j,\varepsilon}_{11}. \tag{2.23}$$

$$F_{V_{i,j},\sigma_3} = m(\sigma_3)\lambda^{\varepsilon}_{V_{i,j},\sigma_3}\frac{u^{\varepsilon}_{i,j}}{d_{i,j,\sigma_3}} = \tau^{i,j}_{22,\varepsilon}u^{\varepsilon}_{i,j}, \ \ \tau^{i,j}_{22,\varepsilon} = 2K^{i,j,\varepsilon}_{22}. \tag{2.24}$$

$$F_{V_{i,j},\sigma_4} = m(\sigma_4)\lambda^{\varepsilon}_{V_{i,j},\sigma_4}\frac{u^{\varepsilon}_{i,j}}{d_{i,j,\sigma_4}} = \tau^{i,j}_{11,\varepsilon}u^{\varepsilon}_{i,j}, \ \ \tau^{i,j}_{11,\varepsilon} = 2K^{i,j,\varepsilon}_{11}. \tag{2.25}$$

So, from (2.6)-(2.19), (2.22)-(2.25) one has the following equations:
1. For $i = 1$ and $2 \leq j \leq N-1$, σ_4 is a boundary edge,

$$-\tau^{1,j-1}_{22,\varepsilon}u^{\varepsilon}_{1,j-1} - \tau^{2,j}_{11,\varepsilon}u^{\varepsilon}_{2,j} - \tau^{1,j+1}_{22,\varepsilon}u^{\varepsilon}_{1,j+1} + \left(\tau^{1,j}_{11,\varepsilon} + \tau^{1,j-1}_{22,\varepsilon} + \tau^{2,j}_{11,\varepsilon} + \tau^{1,j+1}_{22,\varepsilon}\right)u^{\varepsilon}_{1,j} = h^2 f_{1,j}. \tag{2.26}$$

2. For $i = 1$ and $j = 1$, σ_1 and σ_4 are boundary edges,

$$-\tau^{2,1}_{11,\varepsilon}u^{\varepsilon}_{2,1} - \tau^{1,2}_{22,\varepsilon}u^{\varepsilon}_{1,2} + \left(\tau^{1,1}_{11,\varepsilon} + \tau^{1,1}_{22,\varepsilon} + \tau^{2,1}_{11,\varepsilon} + \tau^{1,2}_{22,\varepsilon}\right)u^{\varepsilon}_{1,1} = h^2 f_{1,1}. \tag{2.27}$$

3. For $i = 1$ and $j = N$, σ_3 and σ_4 are boundary edges,

$$-\tau^{1,N-1}_{22,\varepsilon}u^{\varepsilon}_{1,N-1} - \tau^{2,N}_{11,\varepsilon}u^{\varepsilon}_{2,N} + \left(\tau^{1,N}_{11,\varepsilon} + \tau^{1,N-1}_{22,\varepsilon} + \tau^{2,N}_{11,\varepsilon} + \tau^{1,N}_{22,\varepsilon}\right)u^{\varepsilon}_{1,N} = h^2 f_{1,N}. \tag{2.28}$$

4. For $i = N$ and $2 \leq j \leq N-1$, σ_2 is a boundary edge,

$$-\tau^{N-1,j}_{11,\varepsilon}u^{\varepsilon}_{N-1,j} - \tau^{N,j-1}_{22,\varepsilon}u^{\varepsilon}_{N,j-1} - \tau^{N,j+1}_{22,\varepsilon}u^{\varepsilon}_{N,j+1} + \left(\tau^{N-1,j}_{11,\varepsilon} + \tau^{N,j-1}_{22,\varepsilon} + \tau^{N,j}_{11,\varepsilon} + \tau^{N,j+1}_{22,\varepsilon}\right)u^{\varepsilon}_{N,j} = h^2 f_{N,j}. \tag{2.29}$$

5. For $i = N$ and $j = 1$, σ_1 and σ_2 are boundary edges,

$$-\tau^{N-1,1}_{11,\varepsilon}u^{\varepsilon}_{N-1,1} - \tau^{N,2}_{22,\varepsilon}u^{\varepsilon}_{N,2} + \left(\tau^{N-1,1}_{11,\varepsilon} + \tau^{N,1}_{22,\varepsilon} + \tau^{N,1}_{11,\varepsilon} + \tau^{N,2}_{22,\varepsilon}\right)u^{\varepsilon}_{N,1} = h^2 f_{N,1}. \tag{2.30}$$

6. For $i = N$ and $j = N$, σ_2 and σ_3 are boundary edges,

$$-\tau^{N-1,N}_{11,\varepsilon}u^{\varepsilon}_{N-1,N} - \tau^{N,N-1}_{22,\varepsilon}u^{\varepsilon}_{N,N-1} + \left(\tau^{N-1,N}_{11,\varepsilon} + \tau^{N,N-1}_{22,\varepsilon} + \tau^{N,N}_{11,\varepsilon} + \tau^{N,N}_{22,\varepsilon}\right)u^{\varepsilon}_{N,N} = h^2 f_{N,N}. \tag{2.31}$$

7. For $j = 1$ and $2 \leq i \leq N-1$, σ_1 is boundary edge,

$$-\tau^{i-1,1}_{11,\varepsilon}u^{\varepsilon}_{i-1,1} - \tau^{i+1,1}_{11,\varepsilon}u^{\varepsilon}_{i+1,1} - \tau^{i,2}_{22,\varepsilon}u^{\varepsilon}_{i,2} + \left(\tau^{i-1,1}_{11,\varepsilon} + \tau^{i,1}_{22,\varepsilon} + \tau^{i+1,1}_{11,\varepsilon} + \tau^{i,2}_{22,\varepsilon}\right)u^{\varepsilon}_{i,1} = h^2 f_{i,1}. \tag{2.32}$$

8. For $j = N$ and $2 \leq i \leq N-1$, σ_3 is boundary edge,

$$-\tau^{i-1,N}_{11,\varepsilon}u^{\varepsilon}_{i-1,N} - \tau^{i,N-1}_{22,\varepsilon}u^{\varepsilon}_{i,N-1} - \tau^{i+1,N}_{11,\varepsilon}u^{\varepsilon}_{i+1,N} + \left(\tau^{i-1,N}_{11,\varepsilon} + \tau^{i,N-1}_{22,\varepsilon} + \tau^{i+1,N}_{11,\varepsilon} + \tau^{i,N}_{22,\varepsilon}\right)u^{\varepsilon}_{i,N} = h^2 f_{i,N}. \tag{2.33}$$

From (2.20)-(2.33) we get (see [3] and [4]) the following linear equation.

$$K^{\varepsilon h}\, u^{\varepsilon h} = f^h, \tag{2.34}$$

where

$$u^{\varepsilon h} = \begin{pmatrix} u^{\varepsilon}_{1,1} \\ u^{\varepsilon}_{2,1} \\ \vdots \\ u^{\varepsilon}_{N-1,N} \\ u^{\varepsilon}_{N,N} \end{pmatrix}, \quad f^h = h^2 \begin{pmatrix} f_{1,1} \\ f_{2,1} \\ \vdots \\ f_{N-1,N} \\ f_{N,N} \end{pmatrix}, \tag{2.35}$$

$K^{\varepsilon\, h}$ is a square matrix of order N^2.

Note. Throughout the paper, we will denote by c generic constants, even if they take different values at different places. For simplification reasons we adapt the following notations: V and W designate one or the other of the volumes $V_{i,j}(1 \leq i, j \leq N)$.
When V designates one of the volumes $V_{i,j}(1 \leq i, j \leq N)$: (x_V, y_V) designates (x_i, y_j). For any function v, $v(x_V, y_V)$ designates $v(x_i, y_j)$ and v_V designates v_{ij}.

Theorem 2.1. *Let Ω_h be an admissible an uniform mesh of Ω, in the sens of Definition 2.1, such that:*
1) The discontinuities of tensor K^ε coincide with the interfaces of volumes V of Ω_h,
2) $K_{ll} \in C^1\left(\overline{V}\right)$ and $f \in C^1\left(\overline{V}\right)$, for all $V \in \Omega_h$, $l = 1, 2$.

Let $e^{\varepsilon}_V = u^{\varepsilon}(x_V, y_V) - u^{\varepsilon h}_V$, $e^{\varepsilon,*}_V = u(x_V, y_V) - u^{\varepsilon}_V$, where u^ε is the solution of Problem (2.1), u is the solution of Problem (2.2) and $u^{\varepsilon h}$ is the solution of (2.34). Then there exists a constant c independent of ε and h such that:

$$\sum_{\sigma \in \partial\Omega_h} \frac{(\mathcal{D}_\sigma e^\varepsilon)^2}{d_\sigma} m(\sigma) \leq \frac{c\,h^2}{\varepsilon}, \tag{2.36}$$

$$\sum_{V \in \Omega_h} (e^{\varepsilon}_V)^2\, m\,(V) \leq \frac{c\,h^2}{\varepsilon}, \tag{2.37}$$

$$\sum_{\sigma \in \Omega_h} (e^{\varepsilon,*}_V)^2\, m\,(V) \leq \frac{c\,h^2}{\varepsilon} + c\varepsilon, \tag{2.38}$$

where: $\mathcal{D}_\sigma e^\varepsilon = |e^\varepsilon_V - e^\varepsilon_W|$ for $\sigma \in \partial\Omega^{int}_h, \sigma = W|V$, and $\mathcal{D}_\sigma e^\varepsilon = |e^\varepsilon_W|$ for $\sigma \in \partial\Omega^{ext}_h \cap \partial W$, $\partial\Omega^{int}_h$ and $\partial\Omega^{ext}_h$ denote respectively the set of interior and exterior edges of $\partial\Omega_h$.

Proof. To prove the theorem 2.1 we use the same approach as in [13] (Theorem 3.8, p.83, and Theorem 2.3) and [20] (Theorem 1, p. 37). We notice:

$$F^{*,\varepsilon}_{W,\sigma} = \tau^{\varepsilon}_{\sigma}\left(u^\varepsilon(x_V) - u^\varepsilon(x_W)\right) \text{ for } \sigma \in \partial\Omega^{int}_h, \sigma = W|V, \tag{2.39}$$

$$F^{*,\varepsilon}_{W,\sigma} = \tau^{\varepsilon}_{\sigma}\left(-u^\varepsilon(x_W)\right) \text{ for } \sigma \in \partial\Omega^{ext}_h \cap \partial W, \tag{2.40}$$

where τ^ε_σ designates one or the other of the coefficients $\tau^{i,j}_{ll,\varepsilon}(l = 1, 2,\ 1 \leq i, j \leq N)$.
By using Taylor expansions and the same technique as in the 1D (see [20], Theorem 1, p. 37

and [13], Theorem 3.8, p.83) and by using ([2]) (Theorem 2, inequalities (15)-(17)) and [18] (lemma 7.1, p. 163), on can shows that, there exists c such that

$$F_{W,\sigma}^{*,\varepsilon} - \int_{\sigma} -K_W^{\varepsilon} \nabla u^{\varepsilon}(x).n_{W,\sigma} d\gamma(x) = R_{W,\sigma}^{\varepsilon}, \text{ with } |R_{W,\sigma}^{\varepsilon}| \leq \frac{ch^2}{\varepsilon}. \tag{2.41}$$

By integrating the first equation of (2.1) over each control volume, subtracting to (2.5) and using (2.41), one obtains

$$-\sum_{\sigma \in \partial W} G_{W,\sigma}^{\varepsilon} = \sum_{\sigma \in \partial W} R_{W,\sigma}^{\varepsilon}, \ \forall \in \Omega_h. \tag{2.42}$$

where

$$G_{W,\sigma}^{\varepsilon} = \tau_{\sigma}^{\varepsilon} \left(e_V^{\varepsilon} - e_W^{\varepsilon} \right) \text{ for } \sigma \in \partial \Omega_h^{int}, \sigma = W|V, \tag{2.43}$$

$$G_{W,\sigma}^{\varepsilon} = \tau_{\sigma}^{\varepsilon} \left(-e_W^{\varepsilon} \right) \text{ for } \sigma \in \partial \Omega_h^{ext} \cap \partial W. \tag{2.44}$$

To use the same technique as in [13] (Theorem 3.3, p.52), let us multiply (2.44) by e_W^{ε}, sum over $W \in \Omega_h$, and use the conservativity of the scheme, which yields that if then $\sigma = W|V$ $R_{W,\sigma}^{\varepsilon} = -R_{V,\sigma}^{\varepsilon}$. A reordering of the summation over $\sigma \in \Omega_h$ yields the estimate (2.36). From the following discrete Poincaré inequality (see [13]),

$$\sum_{V \in \Omega_h} \left(e_V^{\varepsilon} \right)^2 m\left(V \right) \leq c \sum_{\sigma \in \partial \Omega_h} \frac{\left(\mathcal{D}_{\sigma} e^{\varepsilon} \right)^2}{d_{\sigma}} m(\sigma),$$

yields the L^2 estimate (2.37).
Theory from [6] and [17] on the estimate of the difference $u^{\varepsilon} - u$ with u homogenized solution (Problem 2.2) implies

$$\left\| u^{\varepsilon} - u \right\|_{L^2(\Omega)} \leq c\varepsilon. \tag{2.45}$$

From (2.37) and (2.45) one gets (2.38). ∎

3. NUMERICAL SIMULATIONS

In this section, we are going to present numerical experiments obtained by solving linear system (2.34), and compare them with the solution of homogenized problem (2.2). Two test problems (isotropic and anisotropic cases)will be considered and the source functions $f(x, y)$ will be chosen so as to have an analytical solution of the homogenized problem.

3.1. **Test Problem 1: isotropic case .**

The first series of tests was carried out with an isotropic distribution of heterogeneities (see figure 2 below).

Figure 2: Test Problem 1: typical cell (on left) and an example of periodic heterogeneous porous medium for $\varepsilon = 1/4$ (on right)

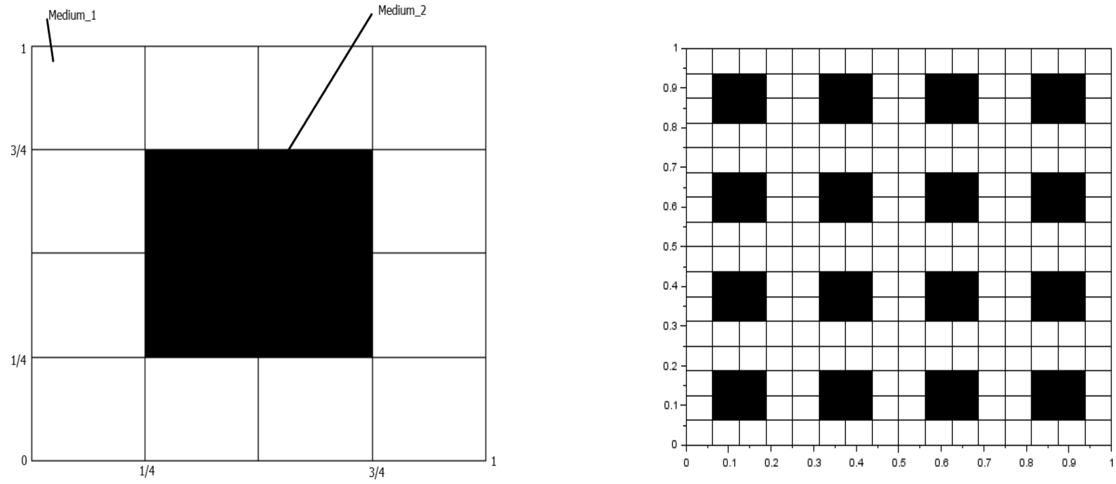

The data are:

Table 3.1: Test Problem 1 data.

Medium_1	Medium_2
$K_{11} = K_{22} = k\ (k > 1)$ $K_{12} = 0$	$K_{11} = K_{22} = 1$ $K_{12} = 0$

3.1.1. *Test 1.* The first test involves simulations with $k = 10$, the effective tensor is [1]: $K^* = 6.52\, I$, where I is the unit matrix. $f\,(x, y) = (K^*_{11} + K^*_{22})\,\pi^2 \sin(\pi x)\sin(\pi y),\ \ (x, y) \in \,]0, 1[\times\,]0, 1[$. So the homogenized solution is: $u(x, y) = \sin(\pi x)\sin(\pi y)$.

Figure 3: Test Problem 1: L2-error for $\varepsilon = \frac{1}{4}$, $k = 10$

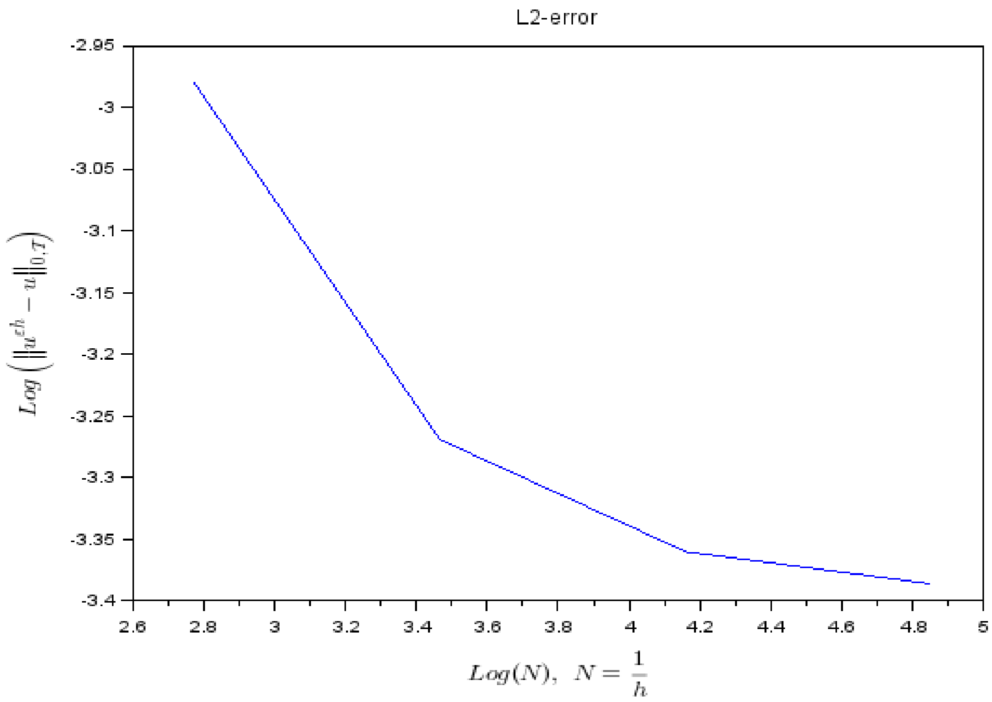

Figure 3 is the error curve obtained by making h tend to 0 and fixing to $\varepsilon = \frac{1}{4}$.

Figure 4: Test problem 1, $\varepsilon = \frac{1}{4}$.

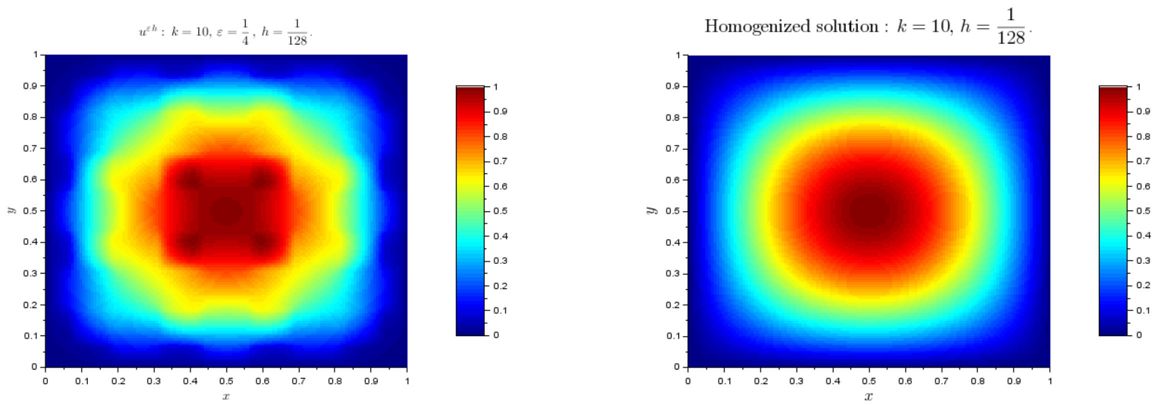

Figure 4 is the representation of $u^{\varepsilon,h}$ and the homogenized solution for the indicated data. It clearly shows that when $\varepsilon = \frac{1}{4}$, Problem (2.1) can be not remplaced by Problem (2.2).

Figure 5: Test problem 1: L2-error for $\varepsilon = \frac{1}{8}$ *and* $k = 10$.

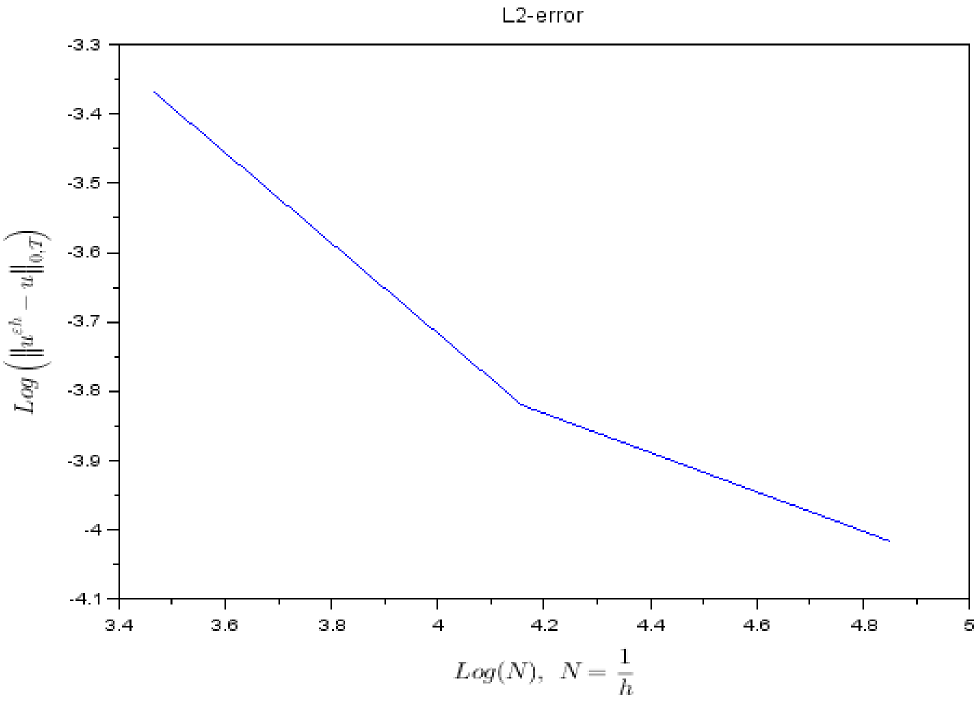

Figure 5 is the error curve obtained by letting h tend to 0, for $\varepsilon = \frac{1}{8}$.

Figure 6: Test problem 1: $\varepsilon = \frac{1}{8}$.

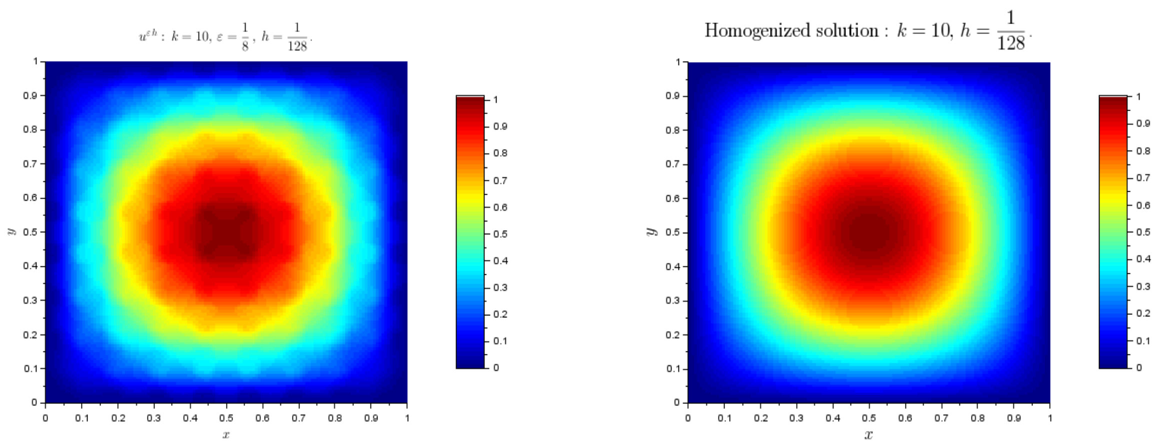

Figure 6 is the representation of $u^{\varepsilon,h}$ and the homogenized solution for the indicated data. It clearly shows that when ε decreases the solution of Problem (2.1) approaches the solution of Problem (2.2).

Table 3.2: Test Problem 1: $k = 10$, $h = \frac{1}{128}$.

$h = \frac{1}{128}$	$\varepsilon = \frac{1}{2}$	$\varepsilon = \frac{1}{4}$	$\varepsilon = \frac{1}{8}$	$\varepsilon = \frac{1}{16}$
$\left\|u^{\varepsilon h} - u\right\|_{0,\Omega_h}$	7.625592e-02	3.384378e-02	1.802047e-02	1.621357e-02

Table 3.2 is obtained by fixing h and making ε tend to 0. The goal is to see how the estimate (2.38) behaves numerically.

Figure 7: Test problem 1: $\varepsilon = \frac{1}{2}$.

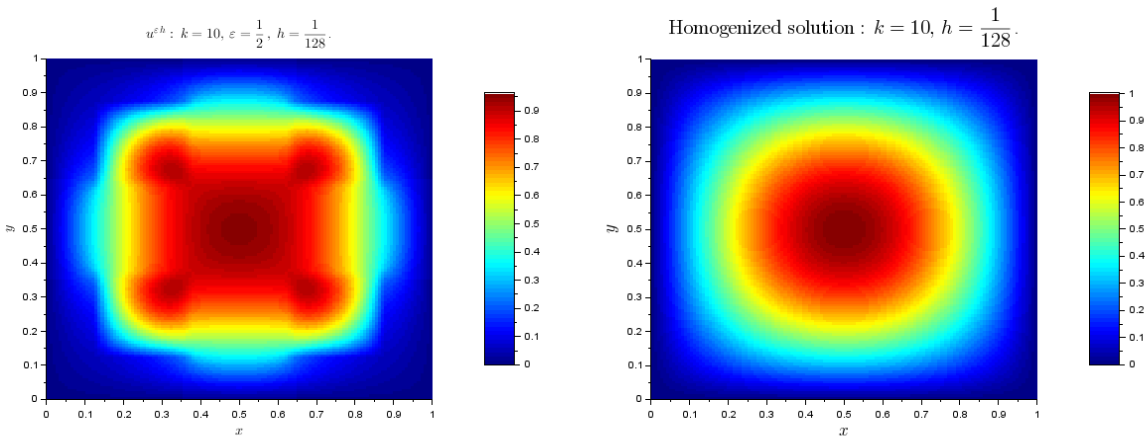

Figure 8: Test problem 1: $\varepsilon = \frac{1}{32}$.

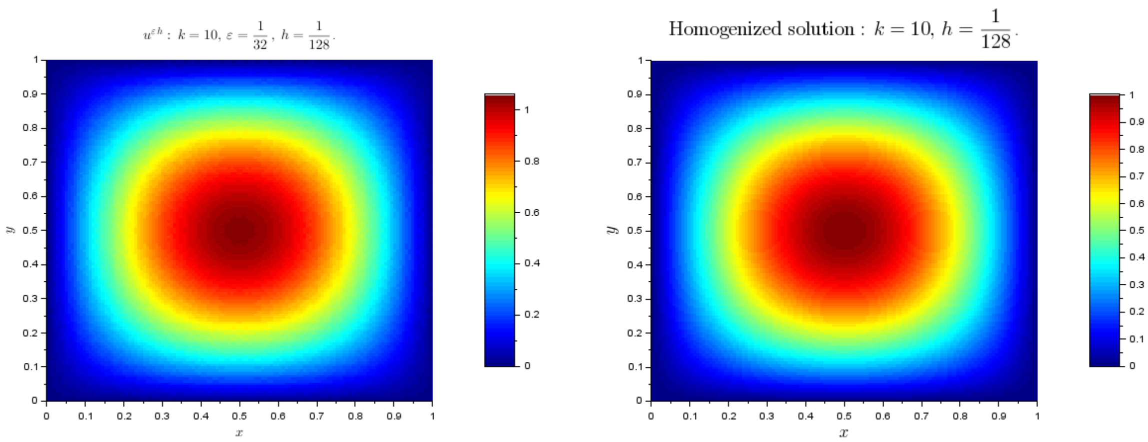

Figures 7 and 8, confirm what when ε decreases the solution of Problem (2.1) approaches the solution of Problem (2.2).

3.1.2. *Test 2.* The second test involves simulations with $k = 100$. In this case the effective tensor is: $K^* = 59.23\, I$ ([1]). The source function f and the homogenized solution remain the same as the paragraph 3.1.1. The results obtained (see Figures 9, 10 & 11) are similar to those obtained in paragraph 3.1.1 with however an impact of the discontinuity jump (see Table 3.3 vs 3.2).

Figure 9: Test problem 1: L2-error for $\varepsilon = \frac{1}{4}, \quad k = 100$

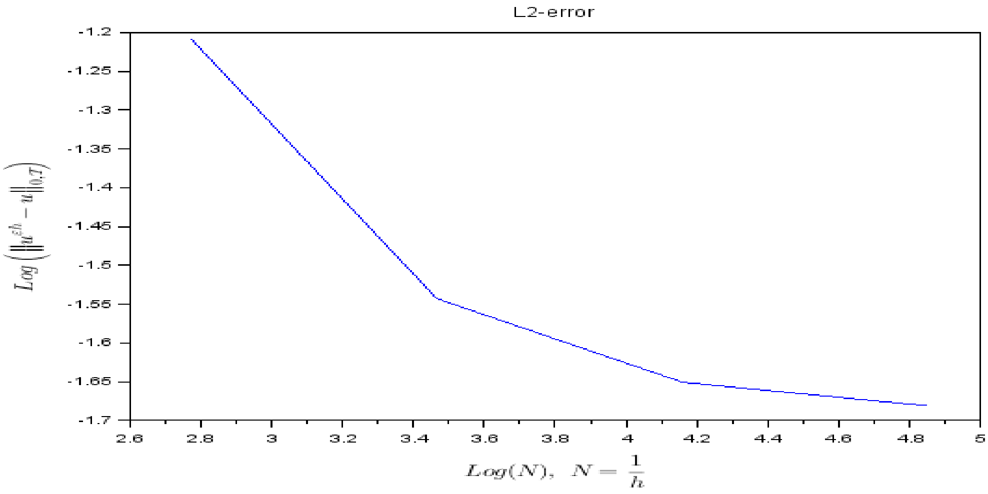

Table 3.3: Test Problem 1: $k = 100$, $h = \frac{1}{128}$.

$h = \frac{1}{128}$	$\varepsilon = \frac{1}{2}$	$\varepsilon = \frac{1}{4}$	$\varepsilon = \frac{1}{8}$	$\varepsilon = \frac{1}{16}$
$\left\|u^{\varepsilon h} - u\right\|_{0,\Omega_h}$	7.089443e-01	1.862146e-01	5.594215e-02	3.252017e-02

Figure 10: Test problem 1: $\varepsilon = \frac{1}{8}$

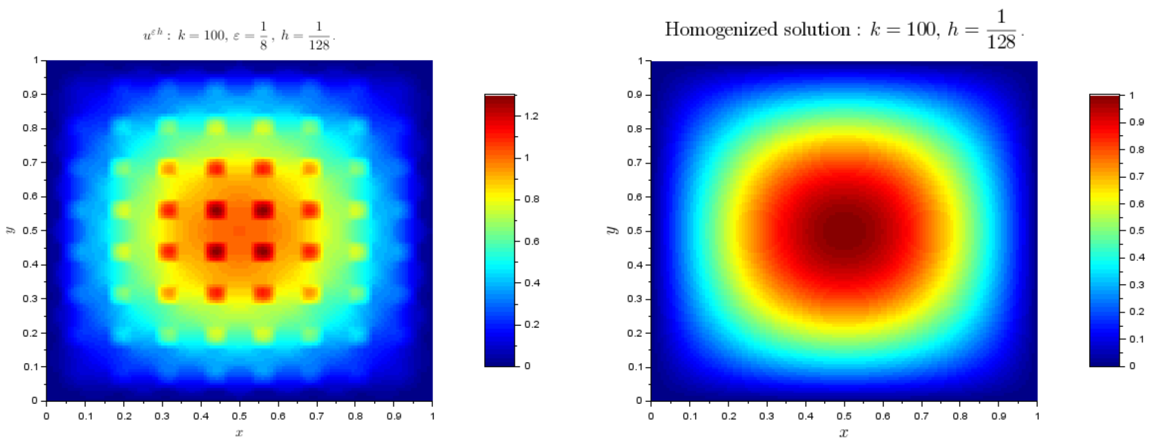

Figure 11: Test problem 1: $\varepsilon = \frac{1}{32}$

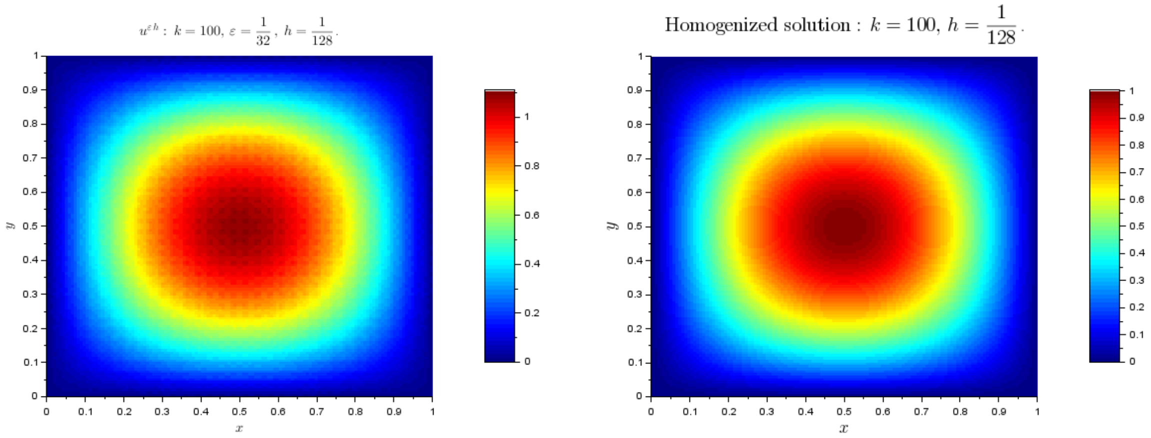

3.2. **Test problem 2: anisotropic case.** The second series of tests was carried out with an anisotropic distribution of heterogeneities (see Figure 12 & Table 3.4 below). The results obtained are globally similar to the isotropic case (see Figure 13 - Figure 18 and Table 3.5 - Table 3.6) with, however a certain impact of the anisotropy ratio on the numerical solution, which is a known phenomenon on methods such as that of finite volumes or finite elements (see e.g. [19]).

Figure 12: Test problem 2: typical cell (on left) and an example of periodic heterogeneous porous medium for $\varepsilon = 1/5$ *(on right)*

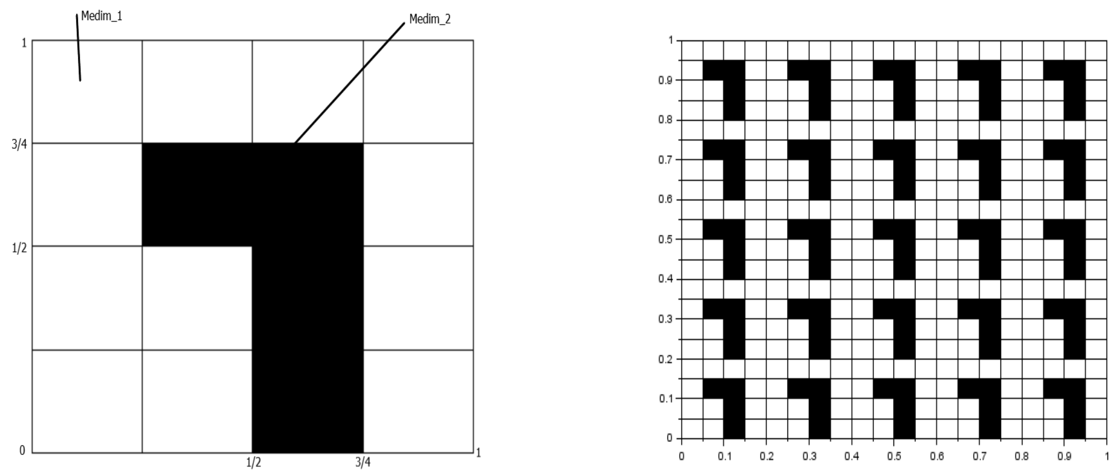

Table 3.4: Test Problem 2 data.

Medium_1	Medium_2
$K_{11} = K_{22} = 1$ $K_{12} = 0$	$K_{11} = K_{22} = k \; (k > 1)$ $K_{12} = 0$

3.2.1. *Test 1.* The first test involves simulations with $k = 10$, the effective tensor is [1]:

$$K^* = \begin{pmatrix} 1.49 & -0.08 \\ -0.08 & 1.89 \end{pmatrix},$$

$$f(x, y) = (K^*_{11} + K^*_{22})\,\pi^2 \sin(\pi x)\sin(\pi y) - 2\,K^*_{12}\pi^2 \cos(\pi x)\cos(\pi y)\ (x, y) \in \,]0, 1[\, \times \,]0, 1[\,.$$

So the homogenized solution is: $u(x, y) = \sin(\pi x)\sin(\pi y)$.

Figure 13: Test problem 2: L2-error for $\varepsilon = \frac{1}{8}, \quad k = 10$

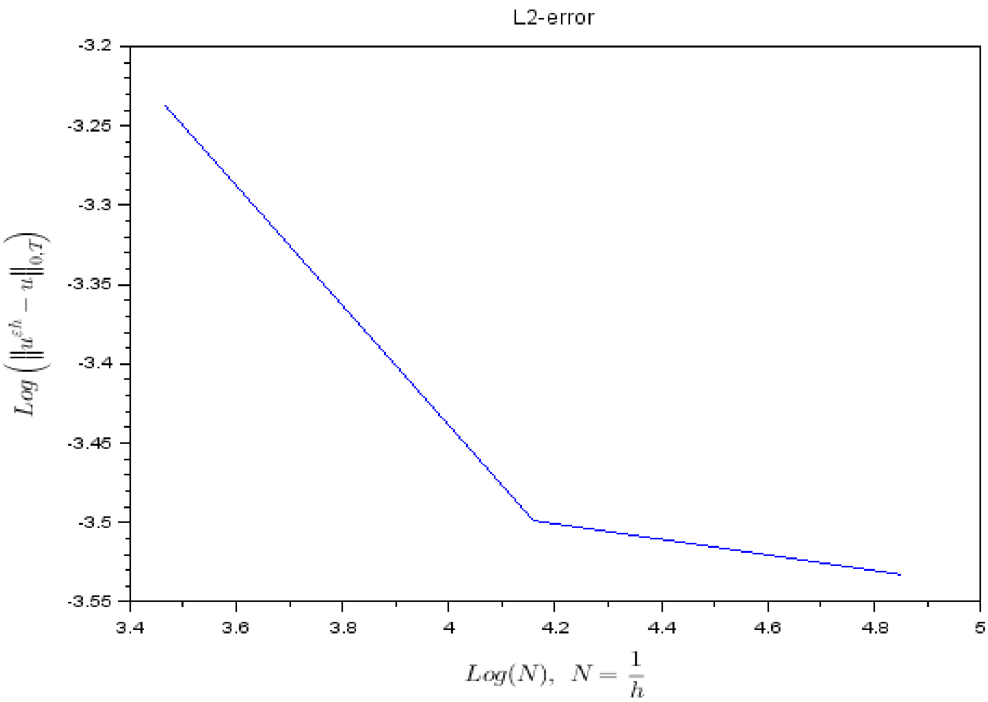

Table 3.5: Table 3 : Test Problem 2: $k = 10$, *and* $h = \frac{1}{128}$.

$h = \frac{1}{128}$	$\varepsilon = \frac{1}{2}$	$\varepsilon = \frac{1}{4}$	$\varepsilon = \frac{1}{8}$	$\varepsilon = \frac{1}{16}$
$\left\|u^{\varepsilon h} - u\right\|_{0,\Omega_h}$	1.038531e-01	5.763713e-02	2.922571e-02	1.957557e-02

Figure 14: Test problem 2: $\varepsilon = \frac{1}{2}$

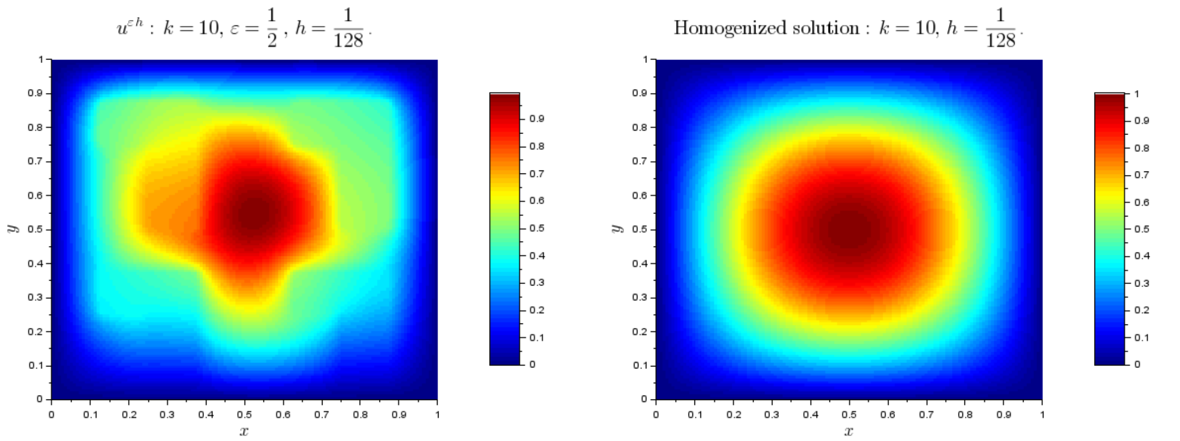

Figure 15: Test problem 2: $\varepsilon = \frac{1}{32}$

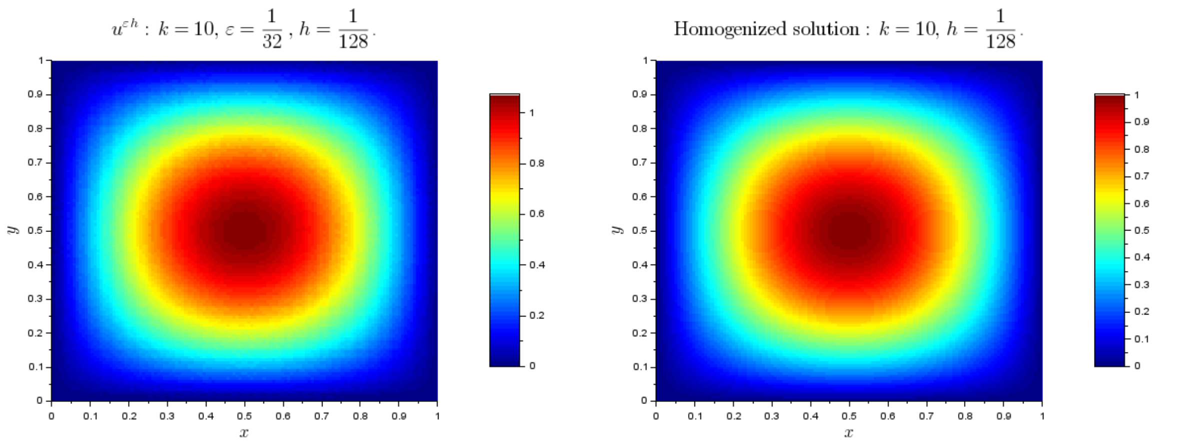

3.2.2. *Test 2.* The second test involves simulations with $k = 100$. In this case the effective tensor is [1]:

$$K^* = \begin{pmatrix} 1.66 & -0.2 \\ -0.2 & 2.57 \end{pmatrix}.$$

The source function f and the homogenized solution remain the same as the test 1.

Table 3.6: Table 4: Test Problem 2: $k = 100$ *and* $h = \frac{1}{128}$

$h = \frac{1}{128}$	$\varepsilon = \frac{1}{2}$	$\varepsilon = \frac{1}{4}$	$\varepsilon = \frac{1}{8}$	$\varepsilon = \frac{1}{16}$
$\left\Vert u^{\varepsilon h} - u \right\Vert_{0,\Omega_h}$	2.275707e-01	1.160337e-01	5.561410e-02	3.630976e-02

Figure 16: Test problem 2: L2-error for $\varepsilon = \frac{1}{8}$, $k = 100$

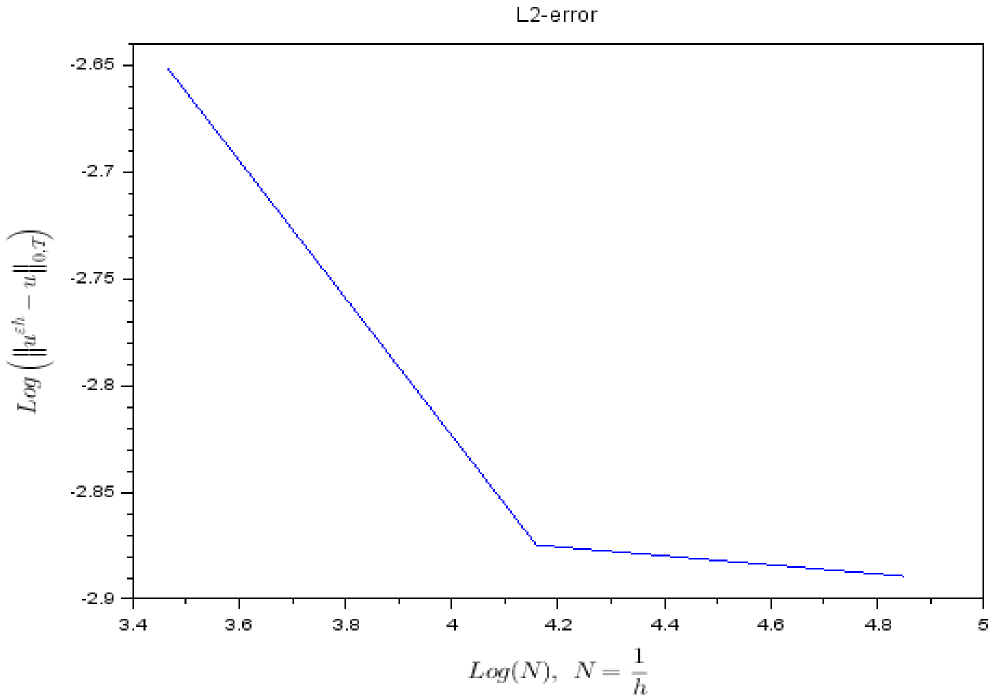

Figure 17: Test problem 2: $\varepsilon = \frac{1}{2}$.

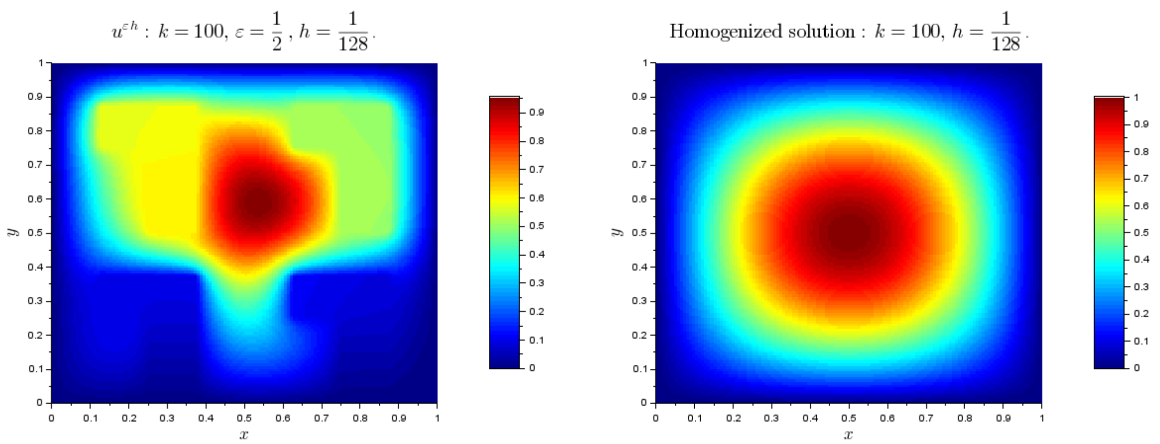

Figure 18: Test problem 2: $\varepsilon = \frac{1}{8}$.

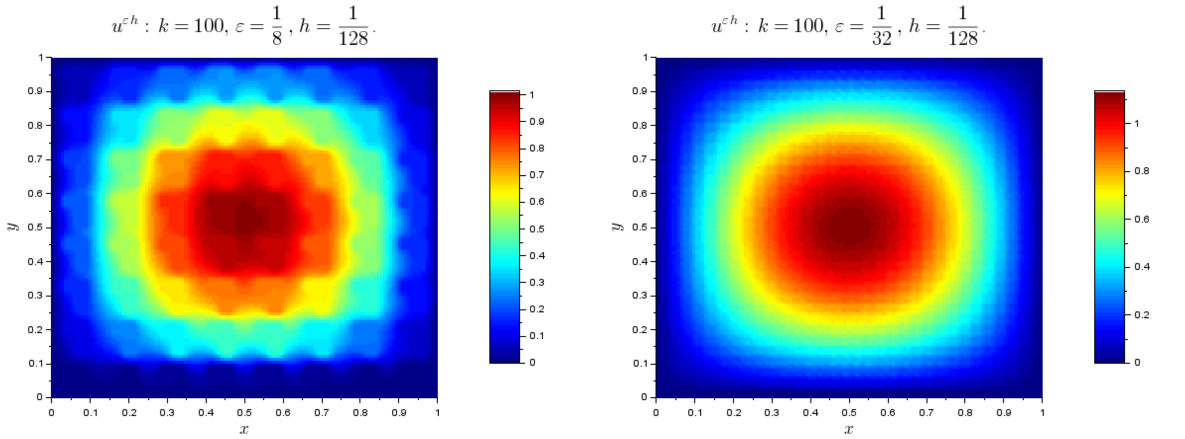

4. Concluding remarks

The aim of this paper was to solve a class of second-order elliptic problems with discontinuous and strongly oscillating coefficients in two dimensions using a finite volume method. For simplicity, the study was limited to the piecewise constant diagonal matrix. The extension of these results to the complete matrix with piecewise continuous coefficients is currently in progress (see [4]). In contrast to the one-dimensional case, which has an analytical solution (see [20] and [22]), enabling a comparison between the approximate and analytical solutions, we used the homogenized solution as a reference solution for the numerical simulations. Consequently, confirming the numerical optimality of the estimate (2.36) remains extremely difficult, particularly in terms of its dependence on ε. However, the results obtained in this article demonstrate, on one hand, the need to directly solve the problem in cases where ε is not small enough because, in these cases, problem (2.1) cannot be replaced by problem (2.2), and on the other hand, the suitability of the finite volume approach for solving the problem.

References

[1] B. AMAZIANE, Global Behavior of Compressible Three-Phase Flow in Heterogeneous Porous Media, *Transport in Porous Media*, **10** (1993), pp. 43–56.

[2] B. AMAZIANE and B. ONDAMI, Numerical approximations of a second order elliptic equation with highly oscillating coefficients, *Notes on numerical Fluid Mechanics*, **70** (1999), pp. 1-11.

[3] J. D. BAMBI PEMBA and B. ONDAMI, Numerical approximation by the method of line with finite-volume approach of a solute transport equationin perioc heterogeneous porous medium, *Aust. J. Math. Anal. Appl.*, **17** (2020), No. 2, Art. 6, 18pp. `https://ajmaa.org/cgi-bin/paper.pl?string=v17n2/V17I2P6.tex`

[4] J. D. BAMBI PEMBA, *Sur l'approximation numérique par une méthode des volumes finis d'une classe d'équations aux derivaes partielles à coefficients fortement oscillants et periodiques*, Thèse de Doctorat. Université Marien NGOUABI, Congo-Brazzaville, 2024.

[5] N. BAKHVALOV and G. PANASENKO, *Homogenization: processes in periodic media*, Mathematics and its Applications, 36, Kluwer, Academic Publishers, London, 1989.

[6] A. BENSOUSSAN, J. L. LIONS and G. PAPANICOLAOUS, *Asymptotic analysis for periodic structures, Studies in Mathematic and its Applications*, 5, North-Holland, Amsterdan, 1987.

[7] J. F. BOURGAT, Numerical experiments of the homogenization method for operators with periodic coefficients, *Rapport de Recherche N^o 277*, INRIA, 1978.

[8] J. F. BOURGAT and A. DERVIEUX, Méthode d'homogénéisation des opérateurs à coefficients périodiques: étude des correcteurs provenant du développement asymptotique, *Rapport de Recherche N^o 278*, INRIA, 1978.

[9] T. CHERNOGOROVA, R. EWING, O. ILIEV and R. LAZAROV, On the Discretization of Interface Problems with Perfect and Imperfect Contact, *Lecture Notes in Physics*, **552** (2000), pp. 93–103. http://dx.doi.org/10.1007/3-540-45467-5_7.

[10] Z. CHEN and T. Y. HOU, A mixed multiscale finite element method for elliptic problems with oscillating coefficients, *Mathematics of computation*, **72** (242)(2002), pp. 541–576. http://dx.doi.org/10.1090/S0025-5718-02-01441-2.

[11] D. ESTEP, M. PERNICE, D. PHAM, S. TAVENER and H. WANG, A posteriori error analysis of a cell-centered finite volume method for semilinear elliptic problems, *Journal of Computational and Applied Mathematics*, **233** (2009), pp. 459–472.

[12] R. EWING, O. P. ILIEV and R. D. LAZAROV, A modified finite volume approximation of second-order elliptic equations with discontinuous coefficients, *SIAM J. Sci. Comp.*, **23** (4)(2001), 1334-1350. http://dx.doi.org/10.1137/S1064827599353877.

[13] R. EYMARD, T. GALLOUËT and R. HERBIN, The finite volume methods, *Handbook of Numerical Analysis, Techniques of Scientific Computing, Part III*, North-Holland, Amsterdam, 2000.

[14] T. GALLOUËT, R. HERBIN and M. H. VIGNAL, Error estimates on the approximate finite volume solution of convection diffusion equations with general boundary conditions, *SIAM Journal on Numerical Analysis*, Vol. 37, No. **6** (2000), pp. 1935–1972.

[15] U. HORNUNG, *Homogenization and porous media*, Interdisciplinary Applied Mathemlatics 6, Springer-Verlag, New York, 1997.

[16] O. ILIEV and I. RYBAK, On Numerical Upscaling for Flows in Heterogeneous Porous Media, *Comput. Methods Appl. Math.*, **8(1)** (2008), pp. 60–76. DOI: 10.2478/cmam-2008-0004, January 2008.

[17] V. V. JIKOV, S. M. KOZLOV and O. A. OLEINIK, *Homogenization of differentials operators and integral functionals*, Springer-Verlag, Berlin, 1994.

[18] O. LADYZHENSKAYA and N. N. URAL'TSEVA, Linear and Quasilinear Elliptic Equations, Leon Ehrenpreis, Academic Press, New York and London, 1968.

[19] P. MAYUR, *Families of Control-Volume Distributed CVD(MPFA) Finite Volume Schemes for the Porous Medium Pressure Equation on Structured and Unstructured Grids*, PhD, Kaunas University of Technology, 2007, https://www.researchgate.net/publication/305810044.

[20] B. ONDAMI, Approximation of a Second-order Elliptic Equation with Discontinuous and Highly Oscillating Coefficients by Finite Volume Methods, *Journal of Mathematics Research*, **8**, no.6 (2016), pp. 34–44. http://www.ccsenet.org/journal/index.php/jmr/article/view/62607.

[21] B. ONDAMI, The Effect of Numerical Integration on the Finite Element Approximation of a Second Order Elliptic Equation with Highly Oscillating Coefficients, *Journal of Interpolation and Approximation in Scientific Computing*, **2** (2015), pp. 128–136.

[22] B. ONDAMI, *Sur quelques problèmes d'homogénéisation des écoulements en milieux poreux*, Thèse de Doctorat. Université de Pau et des Pays de l'Adour, France, 2001.

[23] R. ORIVE and E. ZUAZUA, Finite difference approximation of homogenization problems for elliptic equations Multiscale, *Model. simul.*, **4(1)**(2007), pp. 36–87. http://dx.doi.org/10.1137/040606314.

[24] E. SANCHEZ-PALANCIA, Non-Homogeneous madia and vibration theory, *Lecture Notes in Physics*, 127, Springer-Verlag, Berlin, 1980.

[25] A. A. SAMARSKII, *Theory of Difference Schemes*, Nauka, Moscow, 1977.

[26] A. A. SAMARSKII and V. B. ANDRÉEV, *Méthodes aux Différences pour Équations Elliptiques*, MIR, Moscou, 1978.

[27] H. VERSIEUX and M. SARKIS, Convergence analysis for the numerical boundary corrector for elliptic equations with rapidly oscillating coefficients, *SIAM J. Numer. Anal.* **46(2)**(2008), 545-576. http://dx.doi.org/10.1137/060654773.

[28] H. WEN-MING and C. JUN-ZHI, A new approximate method for second order elliptic problems with rapdly oscillating coefficients based on the method of multiscale asymptotic expansions, *J. Math. Anal.* **335** (2007), 657-668. http://dx.doi.org/10.1016/j.jmaa.2007.01.085.